15

The mechanism of current flow in composite alumochromiun ceramics during its electron beam sintering in a forevacuum

© A.A. Zenin,[1] I.Yu. Bakeev,[1] A.V. Dolgova,[1] A.S. Klimov,[1] E.M. Oks[1,2]

[1] Tomsk State University of Control Systems and Radioelectronics,
634050 Tomsk, Russia
[2] Institute of High Current Electronics, Siberian Branch, Russian Academy of Sciences,
634055 Tomsk, Russia
e-mail: zenin1988@gmail.com

Received August 29, 2022
Revised December 13, 2022
Accepted December 14, 2022

It is shown that during electron beam sintering in the forevacuum pressure region of powder components of composite Al_2O_3-Cr ceramics, the magnitude of the current flowing through the sample depends both on the percentage of chromium and on the heating temperature of the sample. When a certain temperature is reached, the process of current flow is influenced by thermoelectric emission from the sample surface. Along with the ions from the beam plasma, a noticeable thermoelectric emission current contributes to the process of neutralizing the charging of the ceramic surface with an electron beam and reduces the absolute value of the negative potential of the sample surface. This ultimately contributes to an increase in the efficiency of energy transfer from the electron beam to the sample.

Keywords: Electron beam irradiation of oxide ceramics, electrical conductivity, alumina ceramics, chromium, composite, electron beam, forevacuum.

DOI: 10.21883/TP.2023.02.55484.210-22

Introduction

Among the many new structural materials, a special place is occupied by composites based on oxide ceramics [1]. Alumina ceramics due to its mechanical properties, chemical resistance and high operating temperature, and most importantly — easy manufacturing and relative low price, found application in various devices. However, the inherent high brittleness of alumina ceramics limits the possibility of its wider use. It is possible to reduce brittleness by creating composite materials based on such ceramics, for example, by adding metal with close thermophysical properties. One of such promising materials is a composite of alumina ceramics with chromium [2–4]. Composites based on Al_2O_3-Cr have high mechanical strength and are characterized by high resistance to oxidation even at sufficiently high temperatures reaching about 1400°C [5]. Such composites are obtained by sintering powder components in vacuum furnaces at temperatures of 1400–1600°C [6,7]. Recently, alternative methods are actively developed, such as Spark Plasma Sintering (SPS) [8], Selective Laser Sintering (SLM) [9], ultrasonic sintering [10], as well as electron beam sintering [11–13].

During electron-beam sintering of dielectric powders the problem of charge neutralization on the treated surface arises [14]. The use of so-called forevacuum plasma electron sources operating in the pressure range from a few to hundreds of pascals makes it possible to carry out electron-beam processing of dielectrics, including powder sintering, without the use of special means of surface charge compensation [15]. The power of the electron beam used for this method, as well as its position in space, is fairly easy to control. This allows for local heating or heating over a given area of virtually any material. Previously, we shown the fundamental possibility of performing electron-beam sintering of alumina [16] and zirconium [12] ceramics, as well as ceramics based on silicon carbide [17]. During the sintering of ceramics based on silicon carbide, the process of current flow through the sample was studied, and simple considerations were given on the effect of the thermophysical properties of ceramics on the magnitude of this current. In the case of a ceramic composite containing metal, the value of the current flowing through the volume of the sample can be significantly higher, and its maximum values depend on the percentage ratio ceramic–metal. The current flow during electron-beam irradiation of the metal-ceramic composite can significantly change the conditions for charge flow from the irradiated surface. At the same time, the negative potential established on the surface of the irradiated composite can have lower absolute values. This weakens the electron beam deceleration and, accordingly, increases the efficiency of energy transfer to the sample during its electron beam processing. It is important to note that the electric current flowing through the volume of the sintered sample as a result of Joule heating can have a noticeable positive effect directly on the sintering process. The noted circumstances served as the basis for studying the processes of current flow in composite alumochromium ceramics during its electron beam sintering using forevacuum plasma electron sources.

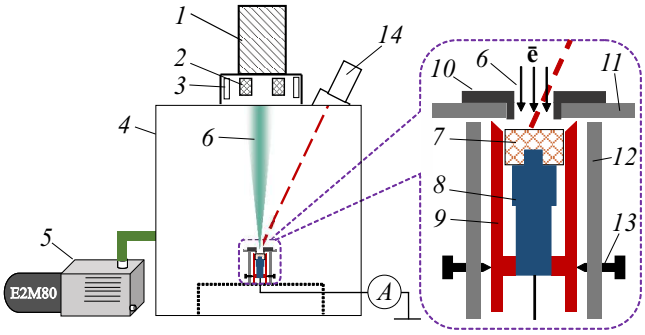

Figure 1. Scheme of the experimental setup: *1* — electron plasma source, *2* — focusing unit, *3* — electron beam deflection and sweep system, *4* — vacuum chamber, *5* — sliding-vane pump, *6* — electron beam, *7* — sintered sample, *8* — current-measuring electrode, *9* — ceramic base, *10* — graphite diaphragm, *11* — massive metal screen, *12* — protective screen, it13 — screws for adjusting and fixing the ceramic base, *14* — pyrometer.

1. Experimental setup

To study the process of current flow during electron-beam sintering of compacted samples of chromium and aluminum oxide powders, a setup was used, the scheme of which is shown in Fig. 1. The forevacuum plasma electron source *1* based on a glow discharge with a hollow cathode [15,18] was mounted on the upper flange of the vacuum chamber *2*. The vacuum chamber was evacuated using a BocEdwards E2M80 mechanical sliding-vane pump. The pump pumping speed provided the required pressure at high gas separation, which occurs during electron-beam heating of a ceramic sample *7*. After reaching pressure of 2–3 Pa, helium of high purity (99.99%) was injected into the vacuum chamber up to working pressure of 30 Pa. Helium ensured the purity of the technological operation of electron-beam heating and the highest electrical strength of the accelerating gap of the plasma source of electrons in comparison with other inert gases.

For the manufacture of ceramic-metal sintered specimens (disk 3 mm thick and 10 mm in diameter), alumina ceramic and chromium powders with average grain sizes of 20 μm were used. The molar ratio of the powder components used in the experiments was as follows: 100% Al_2O_3–0% Cr; 75% Al_2O_3–25% Cr; 50% Al_2O_3–50% Cr; 25% Al_2O_3–75% Cr. The samples were compacted by uniaxial pressing of the powders on a hydraulic press with pressure of 115 MPa with holding under pressure for 5 min.

The current flowing through the sample during heating was measured using special equipment (Fig. 1). The sample to be sintered *7* was located on the current-measuring electrode *8*. To minimize the possibility of the electron beam *6* and beam plasma reaching the current-measuring electrode, the sample was placed in the ceramic base *9*. The current-measuring electrode was protected from high-energy beam electrons by a massive metal screen *11* with a central hole for beam passage, and a graphite diaphragm 10 installed in this hole. The graphite diaphragm is designed to collimate the electron beam and prevent it from reaching the current-measuring electrode *8* and the ceramic base *9*. The hole diameter in the graphite diaphragm is by 2 mm less than the diameter of the sample. Note that there is a gap of 1 mm between the sintered sample of composite ceramics and the graphite diaphragm mounted on the massive metal screen, which provides both electrical and thermal insulation of the sample. To prevent current flow through the ceramic base, there is also a gap between it and the sample. In addition, the geometry of the ceramic base makes it possible to exclude the current flow over the ceramic surface when it is heated to high temperatures. Screws *13* are provided in the design to adjust the entire accessories. To eliminate the influence of plasma and secondary electrons on the measurement results a protective screen *12* is provided in the design.

The sample was sintered using a focused electron beam with a diameter of about 5 mm in the area where it reaches the sample. In the experiments the accelerating voltage, which sets the beam electrons energy, was set at the level of 10 kV, and the electron beam current was smoothly increased from 20 to 100 mA. In this case, the beam power density varied from 1 to 4 kW/cm^2. To ensure uniform heating of the entire surface of the samples under study, the focused and accelerated electron beam was scan into a 15 × 15 mm raster with a scanning frequency of 100 Hz. Under these experimental conditions, visible sputtering of the graphite diaphragm *8* is not observed due to the low specific density of the electron beam power. To measure the temperature of the sample surface irradiated by the electron beam during sintering, RAYTEK 1MH infrared pyrometer with a measurement range from 550 to 3000°C was used, connected to a computer for data acquisition. The current flowing through the sample was measured with an ammeter.

2. Experimental results and discussion thereof

To reduce the thermal stresses arising in ceramics due to its low thermal conductivity, the pressed samples were heated smoothly for 20 min. Throughout the heating, the current flowing through the sample was measured. Fig. 2 shows the dependences of the current flowing through cermet samples on the surface temperature for samples with different chromium content.

On the presented dependences three regions can be distinguished, which differ in the nature of the current change with temperature. Region I corresponds to a relatively low temperature, the current through the sample at such temperatures is small and does not exceed 5% of the maximum current for sample of the corresponding composition. So, for example, for the sample without chromium — 100% Al_2O_3 — the current in the region I

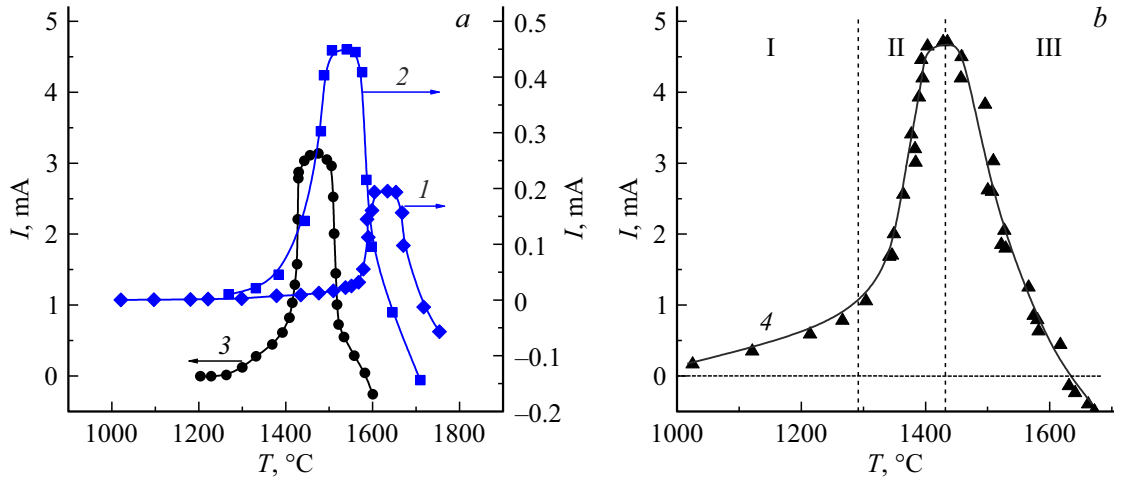

Figure 2. Current vs. temperature of the sample surface during its electron beam irradiation: *a* — samples *1*–*3*, *b* — sample it4 with the designation of characteristic areas. Composition of samples: *1* — 100% Al_2O_3–0% Cr; *2* — 75% Al_2O_3–25% Cr; *3* — 50% Al_2O_3–50% Cr; *4* — 25% Al_2O_3–75% Cr.

does not exceed 10 μA at a maximum in the process of further heating of about 0.2 mA. With the increase in the chromium amount in the sample, the current in region I increases and reaches 1 mA at a temperature of 1200–1250°C (Fig. 2, *b*). This is followed by region II of a much sharper increase in the current up to saturation.

The onset of a sharp increase in the current and its maximum value depend on the chromium content in the sample. The higher the chromium content is, the greater the maximum current is, and the earlier the current rises through the sample starts. For the sample Al_2O_3 without the chromium addition, a significant increase in current is noticeable at temperatures above 1550°C, while for sample with 75% chromium, the current increasing starts at 1000°C. For samples of all compositions the current increasing reaches saturation, and then sharp decrease in the flowing current is observed up to change in its sign (region III).

One of the most probable reasons for the current magnitude decreasing and the change in its direction is thermoelectron emission from the surface of the samples under study. The thermoelectron current is directed opposite to the electron beam current and has a strong dependence on temperature, determined by the well-known Richardson–Dashman relation [19]:

$$j_T = A_0 \cdot T^2 \cdot \exp\left(-\frac{\varphi_V}{k \cdot T}\right), \qquad (1)$$

where A_0 — is thermoelectron constant, $120 \cdot 10^4$ A/(m$^2 \cdot$ K^2), T — sample temperature, φ_V — electron work function.

Fig. 3 shows the experimental dependence of $\ln(I/T^2)$ on $1/T$ for sample with 50% chromium content. The dependence was plotted in the range from 1520 to 1600°C in the descending section of the current through the sample dependence on temperature.

The possibility of plotting a direct dependence of $\ln(I/T^2)$ on $1/T$ (Fig. 3), along with the fact of a smooth current

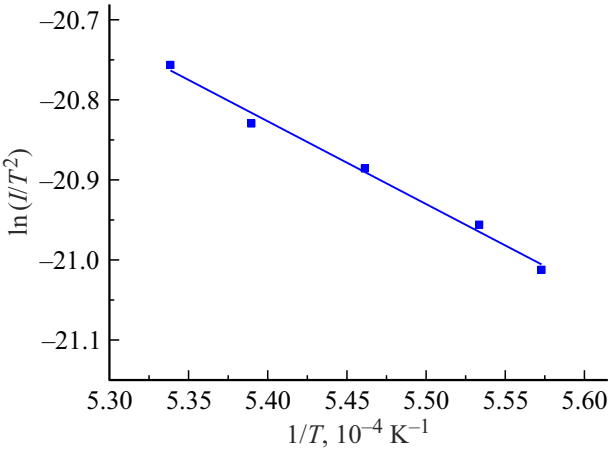

Figure 3. Dependence of $\ln(I/T_2)$ on $1/T$ for sample 50% Al_2O_3–50% Cr.

decreasing when the electron beam is turned off, and the sample cools, is evidence of the thermoelectric emission presence from the surface of the sintered sample. In this case, as follows from the experimental data in Fig. 3, the work function of the composite sample 50% Al_2O_3–50% Cr is about 1.1–1.2 eV.

The explanation of the observed dependences of the current growth on temperature can be as follows. In area I (Fig. 2, *b*), the current is small, since the ceramic component of the composite, being a dielectric, weakly conducts electric current at low temperatures. The chromium particles contained in the composite are located discretely and do not affect the electrical conductivity of the composite. As is known that with the temperature increasing, the electrical conductivity of dielectrics increases, which can lead to increase in the current flowing through the bulk of the sample. The magnitude of the current arising due to

electrical conductivity can be estimated from the ratio

$$I = \gamma ES = \gamma \frac{\Delta U}{h} S, \qquad (2)$$

where γ — electrical conductivity, [S/m]; E — field strength in the sample, [V/m]; S — sample base area, [m2]; ΔU — surface potential, [V]; h — sample thickness.

The field strength in the first approximation is presented as the ratio of the surface potential of the sample to its thickness. Due to the small diameter of the sample, the change in the potential over its surface can be ignored.

Based on (2), the current flowing through the ceramic sample, if we do consider some shrinkage and, accordingly, the change in size during sample sintering, depends on the electrical conductivity and potential on its surface. Moreover, it can be stated with a high degree of certainty that, since aluminum oxide is a dielectric by its nature, the electrical conductivity of samples γ increases exponentially with temperature increasing. The temperature dependence of the potential ΔU and, accordingly, the field strength E can be calculated based on the balance of currents through the sample and the balance of beam plasma particles, with which partial compensation of charging by electron beam of the sintered surface takes place.

The model of the potential formation on the surface of the irradiated sample and the current flowing through its volume during electron-beam sintering is built for the following conditions: the cermet sample is a cylinder with a diameter of $d = 10\,\text{mm}$ and a thickness of $h = 3\,\text{mm}$ from ceramics based on mixture of Al_2O_3-Cr. The electron beam with electron energy $E_0 = 5\,\text{keV}$ and diameter d_b irradiates the flat surface of the sample. Beam electrons, due to the low electrical conductivity of the sample, accumulate on the irradiated surface, which leads to decrease in its potential by value ΔU relative to the grounded holder and the non-irradiated surface. The electron beam propagation in vacuum chamber is accompanied by gas ionization and the formation of a beam plasma. The ions of this plasma are accelerated in the layer separating the beam plasma and the sample surface and fall on the sample, partially compensating the charge accumulated from the beam electrons. Besides, the particles are created due to the ionization of gas atoms by secondary electrons from the sample surface and by thermoelectrons from its heated surface. The beam electrons reflected from the sample also contribute to the ionization. The beam plasma potential φ_p, as a rule, does not exceed a few volts, which is much lower than the possible value of the potential on the surface of the irradiated sample. To simplify the calculations φ_p was taken equal to zero and, thus, the potential difference between the beam plasma and the irradiated surface was assumed to be numerically equal to the potential of the irradiated surface U relative to the potential of the vacuum chamber. The current balance is shown in Fig. 4.

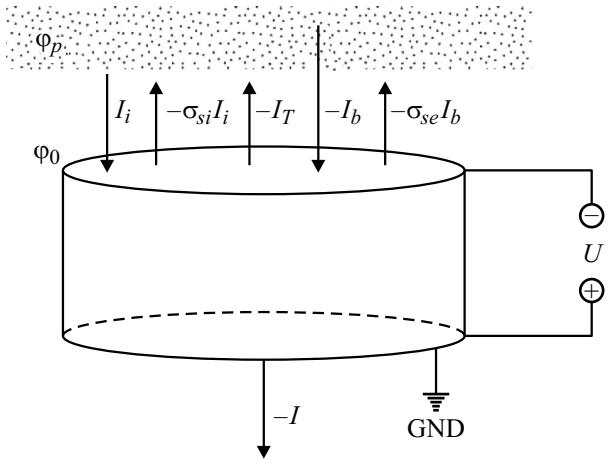

Figure 4. Current balance during irradiation of ceramic sample with electron beam.

The current passing through the sample is determined by the electron beam current I_b, the secondary electron-electron emission current $\sigma_{se} \cdot I_b$, the electron thermal emission current I_T, the current of ions drawn from the plasma I_i and secondary ion-electron emission current $\sigma_{si} \cdot I_i$:

$$I = I_b - \sigma_{se} \cdot I_b - I_T - I_i - \sigma_{si} \cdot I_i, \qquad (3)$$

where σ_{se} — coefficient of secondary electron-electron emission; σ_{si} — secondary ion-electron emission coefficient.

The value of the beam current is determined by the irradiation mode and for the continuous mode was $I_b = 30-100\,\text{mA}$.

Thermal emission current density j_T was calculated using the Richardson–Deshman formula (1) [19]. For each sample composition the work function was calculated in proportion to the content of each component.

The current density of ions j_i from the plasma is determined by the Bohm formula [20]:

$$j_i = 0.4 \cdot e \cdot n_p \sqrt{\frac{2 \cdot k \cdot T}{m_i}} \qquad (4)$$

where n_p — concentration of ions in plasma; $T_e = 11600\,\text{K}$ — electron temperature; $m_i = 6.65 \cdot 10^{-27}\,\text{kg}$ — helium ion mass.

Due to the sufficiently high power of the electron beam and intense thermal radiation the probe measurements are possible only at a considerable distance from the beam axis. The plasma concentration measured in this case will differ significantly from the plasma concentration near the sample. In view of the impossibility of carrying out direct measurements of the plasma concentration in this way, calculation estimates are given that allow one to draw conclusions about the balance of currents supplied to the sample. To find the plasma concentration, the following conditions must be taken into account: ions are produced in plasma due to gas ionization by beam electrons, secondary electrons (they appear due to electron-electron and ion-electron emission), and thermal electrons. The ions leave the plasma to the sintered sample and due to ambipolar

diffusion to the chamber walls in the radial direction. The balance of ions in plasma can be written as follows:

$$\nu_{ib} \cdot n_b + \nu_{is} \cdot (n_{se} + n_{si} + n_T) = \frac{j_i \cdot S}{q_i} \cdot V + D_a \frac{n_p}{L_e^2}, \quad (5)$$

where ν_{ib} — frequency of ionization by beam electrons; n_b — beam electron concentration in plasma; ν_{is} — frequency of ionization by secondary electrons; $n_{se} = \frac{I_b \sigma_{se}}{eS}\sqrt{\frac{m_e}{2eU}}$ — concentration of secondary electrons in plasma formed due to electron-electron emission; $n_{si} = \sigma n_p$ — concentration of secondary electrons in plasma formed due to ion-electron emission; n_T — concentration of thermal electrons in plasma; q_i — ion charge; V — plasma volume, numerically equal to the volume of space occupied by the electron beam; D_a — ambipolar diffusion coefficient; $L_e = \frac{d_b}{\sqrt{2,4}}$ — diffusion length [16].

The frequency of ionization by beam electrons ν_{ib} is a function of the accelerating voltage U_a:

$$\nu_{ib} = n_a \cdot \sigma_i(U_a) \cdot \upsilon(U_a), \quad (6)$$

where n_a — concentration of gas molecules; $\upsilon(U_a)$ — beam electron speed.

The frequency of ionization by secondary electrons ν_{is} is a function of the potential of the irradiated sample surface U:

$$\nu_{is} = n_a \cdot \alpha \cdot (U - U_i) \cdot \exp\left(-\frac{U - U_i}{\beta}\right) \cdot \nu(U), \quad (7)$$

where $U_i = 24.5\,\text{eV}$ — ionization potential for helium α, β — gas type-dependent parameters for helium $\alpha = 0.65 \cdot 10^{-22}\,\text{m}^2/\text{eV}$, $\beta = 160\,\text{V}$.

The beam electron concentration can be defined as

$$n_b(U_a) = \frac{4 \cdot I_b \cdot \sqrt{m_e}}{\pi \cdot d_b^2 \cdot e \cdot \sqrt{2 \cdot e \cdot U_a}}, \quad (8)$$

where m_e is the electron mass.

The concentration of thermal electrons in plasma can be determined similarly:

$$n_t(U) = \frac{4 \cdot I_T \cdot \sqrt{m_e}}{\pi \cdot d^2 \cdot e \cdot \sqrt{2 \cdot e \cdot U}}. \quad (9)$$

The ambipolar diffusion coefficient D_a, taking into account that the ion mobility is much less than the electron mobility $\mu_i \ll \mu_e$:

$$D_a = \frac{\mu_i}{e} \cdot k \cdot (T_e + T_i). \quad (10)$$

Substituting expression (4) into expression (5), taking into account (6)–(10), we can express the concentration of ions in plasma:

$$n_p = L_e^2 \cdot \sqrt{m_i} \cdot \frac{\nu_{ib} \cdot n_b + \nu_{is}(U) \cdot (n_s(U) + n_T(U))}{0.43 \cdot S \cdot L_e^2 \cdot \sqrt{2 \cdot k \cdot T_e} + D_a \cdot \sqrt{m_i}} \cdot V. \quad (11)$$

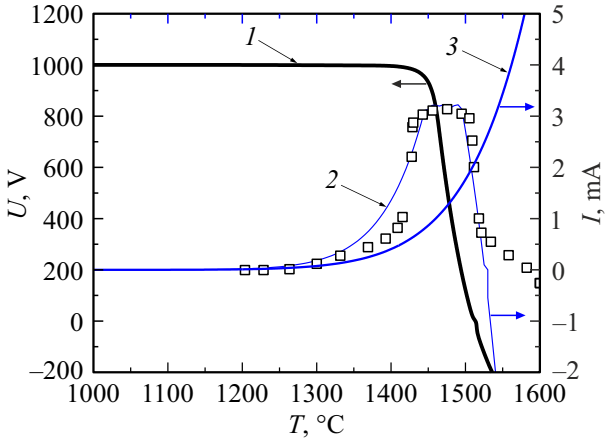

Figure 5. Calculated dependences of the potential (*1*), current through sample (*2*) and the thermal emission current (*3*) for the sample composition 50% Al_2O_3–50% Cr. Experimental current values are represented by dots.

The current passing through the sample is determined by the electrical conductivity, the dependence of which on temperature is largely determined by the temperature dependence of the concentration of charge carriers [21]:

$$\gamma = \gamma_0 \cdot \exp\left(-\frac{\Delta E}{2 \cdot k \cdot T}\right), \quad (12)$$

where γ_0 — conductivity; ΔE — activation energy of conductivity.

Thus, the density of the current passing through the sample due to electrical conductivity:

$$j_\gamma = \gamma_0 \cdot \frac{U}{h} \cdot \exp\left(-\frac{\Delta E}{2 \cdot k \cdot T}\right). \quad (13)$$

Taking into account equations (11)–(13), the current balance can be written in general form:

$$\gamma_0 \cdot \frac{U}{h} \exp\left(-\frac{\Delta E}{2 \cdot k \cdot T}\right) = (1-\sigma_{se}) \cdot j_b - (1+\sigma_{si}) \cdot 0.43 \cdot e \times L_e^2 \cdot \sqrt{2 \cdot k \cdot T_e} \frac{\nu_{ib} \cdot n_b + \nu_{is}(U) \cdot (n_s(U) + n_T(U))}{0.43 \cdot S \cdot L_e^2 \sqrt{2 \cdot k \cdot T_e} + D_a \cdot \sqrt{m_i}} \cdot V - A_0 \cdot T^2 \cdot \exp\left(-\frac{\varphi_V}{k \cdot T}\right). \quad (14)$$

Since the potential cannot be expressed explicitly from expression (14), the potential was calculated using the approximate dichotomy method. The accuracy of the solution was given no worse than 0.1 V. The chromium content in the sample was taken into account by the value of the work function. The result of calculating the potential, the current through the sample and the thermal emission current at the beam electron energy 5 keV, beam current 30 mA for the sample 50% Al_2O_3–50% Cr is shown in Fig. 5.

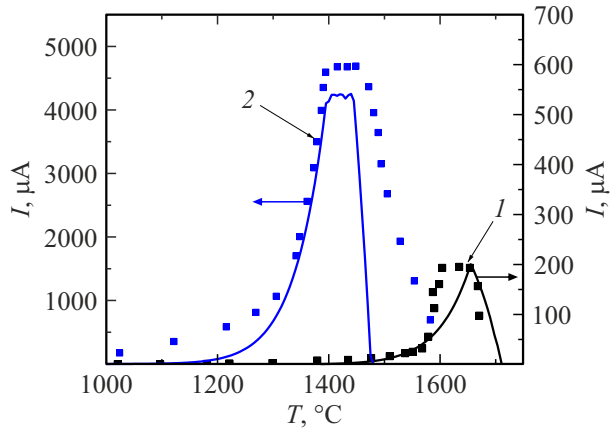

Figure 6. Calculated (solid) and experimental (dots) dependences of the current on the surface temperature during electron beam irradiation for samples of different composition: *1* — 100% Al_2O_3–0% Cr; *2* — 50% Al_2O_3–50% Cr.

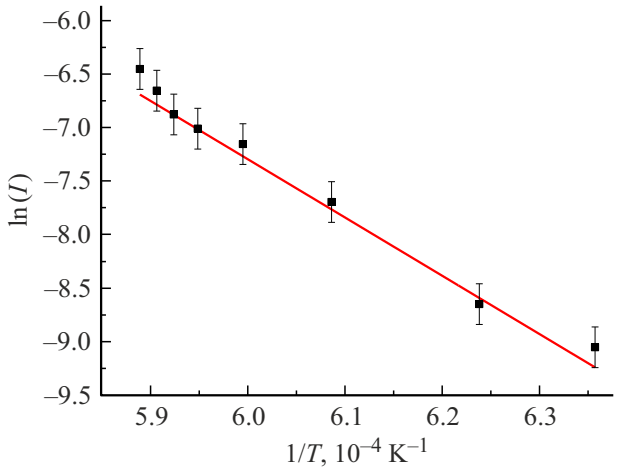

Figure 7. Logarithm of current vs. reciprocal temperature.

As can be seen, at the initial moment of time the negative surface potential U is set at the level of one kilovolt and remains unchanged up to a temperature of 1400°C. The beam electrons are decelerated by this potential and reach the sintered surface with a lower energy. When heating above 1450°C, the absolute value of the negative potential U begins to noticeably decrease. The reason for such potential decreasing is the faster current increasing from the irradiated surface due to thermoelectron emission compared to the current flowing through the sample due to increase in electrical conductivity. The values of the flowing current corresponding to such a dependence of the potential are also shown in Fig. 5. Like the experimental curves (Fig. 2), these dependences contain a section of current growth, then saturation and current decreasing. Based on the dependence of the potential on temperature, we can conclude that the current value is determined by the surface potential, the value of which, in its turn, depends on the balance of currents and particles for the corresponding temperature. And if the beam currents, currents of secondary electron-electron, ion-electron emission, as well as the current of elastically reflected electrons are practically independent of the surface temperature, then the thermal emission current and electrical conductivity change noticeably with temperature increasing. As can be seen from Fig. 4 (curve *3*), at temperature above 1400°C the thermal emission current from the irradiated surface increases, and at temperature of 1540°C becomes comparable to the current through the sample due to electrical conductivity. The thermal electrons carry away the negative charge, which leads to the surface potential decreasing. The surface potential decreasing, according to (13), even at constant electrical conductivity leads to the decrease in current flowing through the sample.

The calculated dependences of the current through the sample as a function of the chromium content are shown in Fig. 6. As can be seen, the trends of the maximum current through the sample change and the shift of the maximum to lower temperatures region coincide with those observed experimentally.

According to the dependence of the current flowing through the sample, it is possible to determine the electrophysical coefficients of the materials used for irradiation. So, in the area of constant potential (Fig. 5) it is possible to calculate the activation energy of conductivity.

Dependence of the logarithm of the current on the reciprocal temperature in the temperature range 1300–1420°C for sample 50% Al_2O_3–50% Cr is shown in Fig. 7. In this temperature range the calculated dependence of the potential is constant, and it can be stated that the increase in current through the sample occurs mainly due to electrical conductivity increasing.

As can be seen, the experimental dependence dots are arranged in straight line. The conductivity activation energy determined from the dependence in Fig. 7, taking into account expression (13), was 4.6 ± 0.4 eV. The value obtained is somewhat lower than the activation energy of pure alumina, but, of course, the presence of an impurity in the form of chromium, and the fact that this energy is determined for a powder material should be taken into account.

Conclusion

The results presented in this paper indicate the need to take into account the effect of electrical conductivity and thermoelectron emission on the processes of electron beam charge compensation during electron beam sintering of composite ceramic compacts. When heating to temperatures close to the optimum sintering temperature, a change in the electrical and physical properties of the composite affects the steady-state potential of the sample surface and, accordingly, the magnitude of the current through the volume of the composite, as well as the efficiency of beam energy transfer to the irradiated surface. The establishment of the potential of the irradiated surface during heating

above 1200°C is significantly affected by thermoelectron emission from the sample surface. The thermoelectron current increasing leads to the potential decreasing to zero and, accordingly, to the termination of the current flow through the volume due to electrical conductivity. The addition of chromium metal powder to the mixture promotes the increase in the current through the sample during electron beam irradiation, but the temperature, at which the surface potential goes to zero, and the current through it stops, decreases. The proposed model of current flow through the sample makes it possible to predict the potential change of composite ceramics during its sintering by electron beam.

Funding

This work was supported by grant FEWM-2020-0038 from the Ministry of Science and Higher Education of the Russian Federation.

Conflict of interest

The authors declare that they have no conflict of interest.

References

[1] J. Huang, P.K. Nayak. Advances in Nanocomposite Technol., **7**, (2011). DOI: 10.5772/17899
[2] J.L. Guichard, O. Tillement, A. Mocellin. J. Europ. Ceramic Society, **18** (12), 1743 (1998).
[3] D. Osso, O. Tillement, A. Mocellin, G. Le Caer, 0. Babushkin, T. Lindback. J. Europ. Ceramic Society, **15** (12), 1207 (1995). DOI: 10.1016/0955-2219(95)00096-8
[4] T.S. Shelvin. J. American Ceramic Society, **37** (3), 140 (1954).
[5] J.L. Guichard, A. Mocellin, M.O. Simonnot, J.F. Remy, M. Sardin. Powder Technol., **99** (3), 257 (1998).
[6] M. Chmielewski, K. Pietrzak. J. Europ. Ceramic Society, **27** (2), 1273 (2007).
[7] Y. Ji, J.A. Yemans. J. Mater. Sci., **37** (24), 5229 (2002).
[8] M. Tokita. Advances Sci. Technol., **63**, 322 (2010).
[9] S.K. Tiwari, S. Pande, S. Agrawal, S.M. Bobade. Rapid Prototyping J., **21** (6), 630 (2015). DOI: 10.1108/RPJ-03-2013-0027.
[10] O. Khasanov, U. Reichel, E. Dvilis, A. Khasanov. IOP Conference Series: Mater. Sci. Engineer., **18** (8), 082004 (2011). DOI: 10.1088/1757-899X/18/8/082004
[11] C.N. Sun, M.C. Gupta, K.M. Taminger. J. American Ceramic Society, **93** (9), 2484 (2010). DOI:10.1111/j.1551-2916.2010.03832.x
[12] V. Burdovitsin, E. Dvilis, A. Zenin, A. Klimov, E. Oks, V. Sokolov, O. Khasanov. Advanced Mater. Res., **872**, 150 (2014).
[13] V.K.V. Pasagada, N. Yang, C. Xu. Ceramics Intern., **48** (7), 10174. DOI: 10.1016/j.ceramint.2021.12.229
[14] A. Kirchner, B. Klöden, J. Luft, T. Weißgärber, B. Kieback. Powder Metall, **58** (4), 246 (2015). DOI: 10.1179/0032589915Z.000000000244
[15] E. Oks. *Plasma Cathode Electron Sources: Physics, Technology, Applications* (Weinheim, Wiley — VCH Verlag GmbH & CO. KGaA, 2006)
[16] A.S. Klimov, I.Y. Bakeev, E.S. Dvilis, E.M. Oks, A.A. Zenin. Vacuum, **169**, 108933 (2019). DOI: 10.1016/j.vacuum.2019.108933
[17] A.S. Klimov, V.A. Burdovitsin, A.A. Zenin, E.M. Oks, O.L. Khasanov, E.S. Dvilis, A.O. Khasanov. Tech. Phys. Lett., **41** (8), 747 (2015). DOI: 10.1134/S1063785015080118
[18] A.A. Zenin, I.Y. Bakeev, A.S. Klimov, E.M. Oks. Plasma Sources Sci. Technol., **30** (3), 035007 (2021). DOI: 10.1088/1361-6595/abe175
[19] S. Dushman. Reviews of Modern Phys., **2** (4), 381. DOI: 10.1103/RevModPhys.2.381
[20] D. Bohm. *The Characteristics of Electrical Discharges in Magnetic Fields* (McGraw-Hill, NY., 1949), p. 77.
[21] H. Ibach, H. Lüth. *Semiconductors. In: Solid-State Physics* (Springer, Berlin, Heidelberg, 2009), DOI: 10.1007/978-3-540-93804-0_12